Mem. S.A.It. Vol. 84, 926

Memorie della

Optical and near-infrared spectroscopy of free-floating planets in the σ Orionis cluster

M. R. Zapatero Osorio[1], V. J. S. Béjar[2,3], and K. Peña Ramírez[2,3]

[1] Centro de Astrobiología (CSIC-INTA), Crta. Ajalvir km 4, 28850 Torrejón de Ardoz, Madrid, e-mail: mosorio@cab.inta-csic.es
[2] Instituto de Astrofísica de Canarias, Vía Láctea s/n, 38205 La Laguna, Tenerife
[3] Departamento de Astrofísica, Universidad de La Laguna, La Laguna, Tenerife

Abstract. We present our spectroscopic follow-up of free-floating planetary-mass candidates of the young (3 Myr), nearby (352 pc), solar metallicity star cluster σ Orionis. Optical and near-infrared low resolution spectra were acquired for a total of 13 faint (J = 18.2–20 mag), cluster free-floating planet candidates using OSIRIS (700–980 nm, $R \sim$ 200–310) on the GTC and ISAAC (1.09–1.42 μm, $R \sim$ 500) on the VLT. We investigated the spectroscopic properties of low-gravity ultracool atmospheres (expected $T_{\rm eff}$ in the range 1000–2300 K, and $\log g \sim$ 3.5), and the candidates membership in the cluster. If confirmed as bona-fide σ Orionis members, their masses would range from 5 through 13 times the mass of Jupiter. These data allowed us to set strong constrains on the σ Orionis planet-mass function that will become a benchmark of substellar mass functions against which to compare findings in different regions of the Galaxy, including the field.

Key words. Stars: brown dwarfs – Stars: luminosity function, mass function.

1. Introduction

Our main goal is to study the substellar mass function of the young σ Orionis cluster (2–8 Myr, 352 pc, solar metallicity; Zapatero Osorio et al. 2002a; Perryman et al. 1997; González Hernández et al. 2008). To this end, bona-fide cluster members have to be identified via photometric, astrometric and spectroscopic observations. Here, we present the spectroscopic follow up of a significant number of known photometric planetary-mass candidates. Because of their expected young age, substellar objects are still undergoing self-contraction; they thus display low-surface gravity atmospheres (see Luhman 2012, and references therein).

2. Target selection

We selected 12 planetary-mass candidates of the σ Orionis cluster recently discovered in the extensive $ZYJHK$ survey of Peña Ramírez et al. (2012), which have no published spectra. One additional candidate, S Ori 70 (T5.5±1; Zapatero Osorio et al. 2002b), was included in the target list shown in Table 1. All 13 targets along with ∼200 cluster low-mass member candidates and the theoretical, solar metallicity, 3-Myr isochrone of Chabrier et al. (2000) are shown in the color-magnitude diagram of Figure 1. Predicted luminosities and effective

Send offprint requests to: M. R. Zapatero Osorio

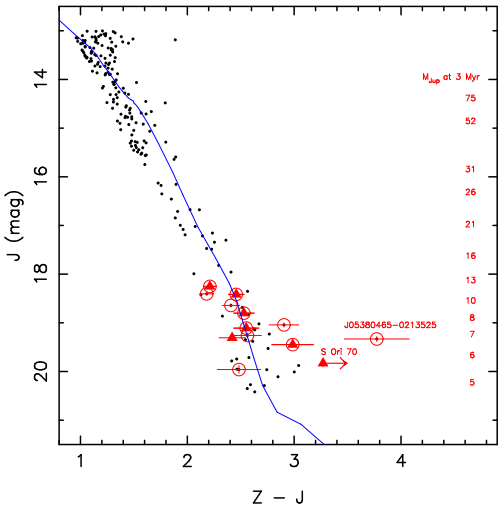

Fig. 1. Color-magnitude diagram of low-mass σ Orionis candidates taken from Peña Ramírez et al. (2012, small dots, VISTA photometry). OSIRIS and ISAAC targets are plotted as solid triangles and open circles. Two T-type objects are labeled. S Ori 70 remains undetected in the VISTA Z-band, and its $Z - J$ lower limit is depicted with an arrow. The 3-Myr isochrone is shown with a solid line. Masses (Jupiter units) predicted by the 3-Myr model are given on the right side of the panel. Photometric error bars are plotted only for our targets.

temperatures were transformed into magnitudes and VISTA colors using literature relations between J-band bolometric corrections, observed $Z - J$ colors, measured surface temperatures, and spectral types (Hewett et al. 2006; Stephens et al. 2009). These relations are valid for temperatures between 3300 K and ~1000 K or spectral types M1–T6. Our program objects have J and $Z - J$ colors in the intervals 18.2–20 mag and 2.2–3.8 mag, respectively. They belong to the faintest tail of cluster member candidates known to date. If confirmed to be true σ Orionis members, their masses would span from the deuterium burning-mass limit at about 13 $M_{\rm Jup}$ (Saumon et al. 1996) down to 5–6 $M_{\rm Jup}$.

3. Observations

Table 1 provides the journal of the optical and near-infrared observations. Seven σ Orionis planetary-mass candidates were observed at optical wavelengths using the OSIRIS spectrograph (Cepa 1998) located at one of the Nasmyth foci of the GTC telescope on Roque de los Muchachos Observatory (La Palma, Spain). The instrumental setup provided data with a nominal dispersion of 7.68 Å pix^{-1}. The slit widths were chosen depending on the seeing conditions. Typical seeing during the observations was 0.″7–1.″0 at optical wavelengths and weather conditions were mainly clear. The binning of the pixels along the spectral direction and the projection of the slits onto the detector yielded spectral resolutions of $R = 200$–310 (widest to narrowest slit) at 750 nm.

J-band near-infrared spectroscopy was obtained for eleven σ Orionis planetary-mass candidates (five of them in common with the optical targets) using the low-resolution grating centered at 1.25 μm, a slit width of 1.″0, and the ISAAC instrument (Moorwood et al. 1998) installed on the Nasmyth A focus of the VLT sited on Cerro Paranal (Chile). This instrumental configuration yielded a spectral nominal dispersion of 3.49 Å pix^{-1}, a resolving power of about 500 at the central frequency, and a wavelength coverage of 1.09–1.42 μm. Typical seeing of the observations ranged from 0.″7 to 1.″0.

OSIRIS and ISAAC spectra were acquired at two nodding positions along the slits separated by 10″ for a proper subtraction of the Earth's sky emission contribution. Both the target and a reference bright star within typically 1′-distance from the program object were centered on the slits. Data were not obtained at parallactic angle, which has no impact at infrared wavelengths. In the visible, targets were acquired onto the slit using the z' filter with a passband of 825–1000 nm; that is we cared that most red flux passed through the slit. In addition, they do not contribute significantly at blue wavelengths (≤650 nm), where the flux loss due Earth's atmospheric refraction would be high. By observing the reference bright stars once at parallactic angle immediately after the targets, we checked that no corrections due to blue-photon losses are required for the OSIRIS program sample.

Table 1. σ Orionis candidates: log of the spectroscopic observations.

Object	J (mag)	Z-J (mag)	Obs. date	Inst./Teles.	Grat.	Slit (")	$\Delta\lambda$ (Å)	$t_{\rm exp}$ (s)
S Ori J05382650−0209257	18.25	2.21	2012 Dec 03	ISAAC/VLT	LR	1.0	1.097–1.339	8×600
			2012 Dec 14	OSIRIS/GTC	R300R	1.2	0.700–0.980	4×1800
S Ori J05382962−0304382	18.40	2.18	2012 Dec 04	ISAAC/VLT	LR	1.0	1.097–1.339	8×600
S Ori J05382951−0259591	18.42	2.46	2012 Dec 01	ISAAC/VLT	LR	1.0	1.097–1.339	10×600
			2012 Dec 13	OSIRIS/GTC	R300R	0.8	0.700–0.980	4×1200
S Ori J05382471−0300283	18.64	2.41	2012 Dec 02	ISAAC/VLT	LR	1.0	1.097–1.339	8×600
S Ori J05382952−0229370	18.80	2.53	2013 Jan 26	ISAAC/VLT	LR	1.0	1.097–1.339	12×600
			2012 Dec 15	OSIRIS/GTC	R300R	1.0	0.700–0.980	3×1200
S Ori J05385751−0229055	19.04	2.90	2012 Dec 01	ISAAC/VLT	LR	1.0	1.097–1.339	8×600
S Ori J05370549−0251290	19.11	2.55	2013 Jan 27	ISAAC/VLT	LR	1.0	1.097–1.339	8×600
			2012 Dec 16	OSIRIS/GTC	R300R	1.0	0.700–0.980	4×1200
S Ori J05380323−0226568	19.26	2.57	2013 Jan 26	ISAAC/VLT	LR	1.0	1.097–1.339	16×600
S Ori J05400004−0240331	19.31	2.42	2012 Dec 15	OSIRIS/GTC	R300R	1.0	0.700–0.980	4×1800
S Ori J05380465−0213525	19.33	3.77	2012 Dec 04	ISAAC/VLT	LR	1.0	1.097–1.339	8×600
S Ori J05380006−0247066	19.45	2.99	2012 Dec 02	ISAAC/VLT	LR	1.0	1.097–1.339	14×600
			2012 Dec 16	OSIRIS/GTC	R300R	1.2	0.700–0.980	4×1800
S Ori 70	19.83	≥3.2	2012 Dec 14	OSIRIS/GTC	R300R	0.8	0.750–0.980	8×1800
S Ori J05382529−0242253	19.96	2.48	2012 Dec 03	ISAAC/VLT	LR	1.0	1.097–1.339	13×600

Raw images were reduced following standard procedures for optical and near-infrared wavelengths. Pairs of nodded frames were subtracted to remove the background emission contribution and then divided by the corresponding flat fields. Since our targets are very faint sources and the trace of their spectra is barely seen in individual exposures, we used the observations of the reference stars to precisely register the two-dimensional spectra. The registered frames were stacked together before optimally extracting the spectra of the targets. The extracted spectra were calibrated in wavelength, corrected for instrumental response and telluric absorption using data of B-type stars (near-infrared) and G 158−100 (white dwarf, optical), which were observed with the same instrumental configurations as the science targets and at similar air masses. Finally, the data were multiplied by black body curves of appropriate temperatures to restore the spectral slope. Some of the resulting spectra are illustrated in Figures 2 and 3.

4. Discussion and final remarks

After comparison of our observations with data acquired with the same instrumental configuration as the science data and on the same observing dates, and with data from the literature, we conclude the following.

The T spectral types of S Ori 70 and S Ori J05380465−0213525 are confirmed. For the later, we derive spectral type T5 ± 0.5 based on the strong water vapor and methane absorptions of its J-band spectrum (Figure 3). The very red slope of the optical spectrum of S Ori 70 (Figure 2) is consistent with spectral type T6. We note that water vapor absorption at ~925 nm is not detected in S Ori 70, in contrast with observations of many other T dwarfs in the field. This might be due to the very low resolution and poor signal-to-noise ratio of the data.

All the remaining objects are Galactic sources since water vapor at 1.33 μm and oxides are clearly detected in the spectra, except for the faintest target S Ori J05382529−0242253. This source does not show the steam feature at 1.33 μm and has very red mid-infrared colors (Peña Ramírez et al. 2012), likely indicating its extragalactic nature. In our sample, extragalactic contamination is quite low (less than 10%). We caution that some model atmospheres predict very weak water vapor absorption at low gravities and very low surface temperatures ($T_{\rm eff} \leq 1400$ K; see e.g., Patience et al. 2012).

With the exception of the T-type sources and J0538−0242, the spectra show clear atomic and molecular signposts of youth. The

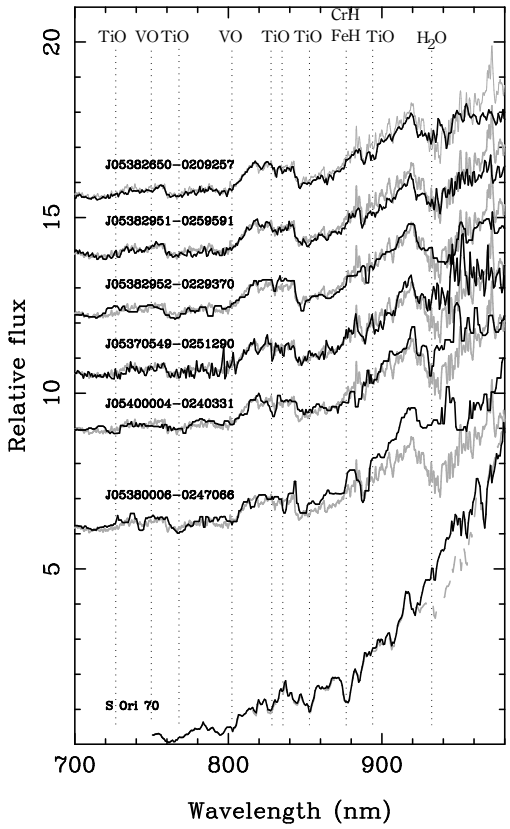

Fig. 2. OSIRIS optical spectra (solid black and dashed lines). The optical spectrum of USco 108B (Béjar et al. 2008) is also shown (gray) for comparison with the top six spectra. Two spectra of S Ori 70 are displayed: the one corrected for telluric absorption (black solid) and the one without telluric correction (dashed line). All data are normalized to unity at 814–817.5 nm and are offset for clarity. Some spectra are smoothed to improve the signal-to-noise ratio. Various molecular features are identified.

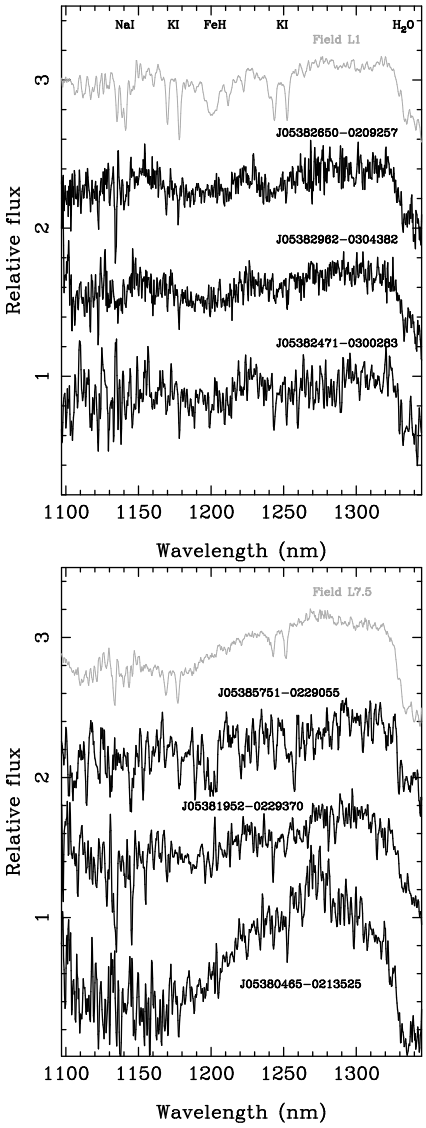

Fig. 3. Some ISAAC spectra of σ Orionis candidates (black) and field dwarfs (gray) obtained with the same instrumental configuration. Data are offset and normalized to unity at 1.28–1.32 μm.

K I lines in the *J*-band appear weaker in our data than in field high-gravity objects of similar surface temperatures (Figure 3), which can be attributed to sub-solar metallicities or low pressure/gravity atmospheres. For those objects with optical and near-infrared spectra, TiO and VO absorptions appear quite strong in the visible, a fact that is opposite to metal underabundances. Therefore, low gravity is the most likely explanation to account for the weak alkali lines and strong oxides, which support cluster membership.

In Figure 4 we compare two of our targets with model spectra by Allard et al. (2011). The models fail to fit the fine details, but the slope from optical to near-infrared wavelengths is

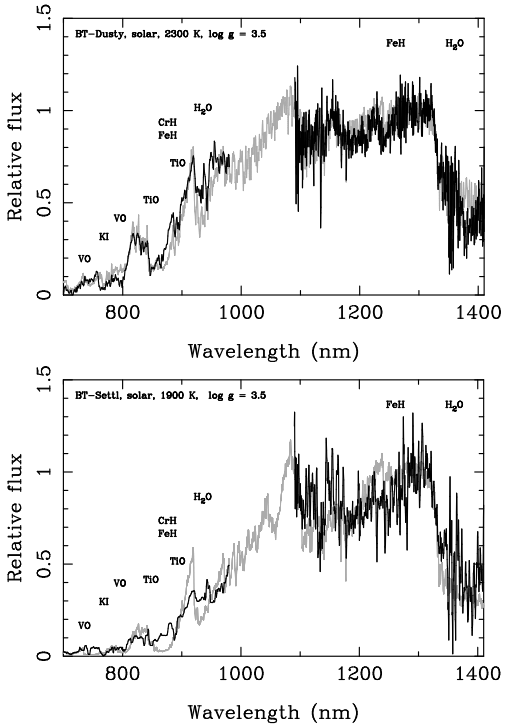

Fig. 4. OSIRIS and ISAAC spectra (black) of J0538−0209 (top) and J0538−0247 (bottom) compared to spectral synthesis (gray) by Allard et al. (2011). Theoretical spectra were degraded to the spectral resolution of the observations. ISAAC data are normalized to unity at 1.28–1.32 μm, and OSIRIS data are normalized to the J-band spectra by using the VISTA $Z - J$ colors.

well reproduced. From these models we infer $T_{\rm eff}$ values between 2300 and 1900 K and $\log g$ of 3.5 for the five sources with both OSIRIS and ISAAC data. We note that only low values of surface gravity were able to explain the observed strength of VO, TiO and K I features. Derived spectroscopic $T_{\rm eff}$'s and surface gravities are in agreement with the 3-Myr isochrone shown in Figure 1 at the 1-σ level. Therefore, estimated masses are 6–13 $M_{\rm Jup}$ as described in Section 2. Our spectroscopic follow-up confirms a large number of σ Orionis planetary-mass objects (about 50% of all candidates with J=19.3–20 mag), providing strong support for the cluster mass function presented in Peña Ramírez et al. (2012). The σ Orionis planetary-mass interval between 6 and 13 $M_{\rm Jup}$ is over-abundant by a factor of 2–5 with respect to the extrapolation of the widely used Chabrier (2005) log-normal mass function.

Acknowledgements. This work is based on observations made with the GTC, installed at the Spanish Observatorio del Roque de los Muchachos of the Instituto de Astrofísica de Canarias, in the island of La Palma. Also based on observations made with ESO Telescopes at the Paranal Observatory under program ID 090.C-0766. This work is partly financed by the Spanish Ministry of Economy and Competitivity through the project AYA2011-30147-C03-03.

References

Allard, F., Homeier, D., & Freytag, B. 2011, in 16th Cambridge Workshop on Cool Stars, Stellar Systems, and the Sun, eds. C.M. Johns-Krull, M.K. Browning, & A.A. West, (San Francisco, ASP), ASP Conf. Ser., 448, 91

Béjar, V. J. S., et al. 2008, ApJ, 673, L185

Cepa, J. 1998, Ap&SS, 263, 369

Chabrier, G. 2005, in The Initial Mass Function 50 Years Later, eds. E. Corbelli, F. Palla, & H. Zinnecker, (Dordrecht: Springer), ASSL, 327, 41

Chabrier, G., Baraffe, I., Allard, F., & Hauschildt, P. H. 2000, ApJ, 542, 464

González Hernández, J. I., et al. 2008, A&A, 490, 1135

Hewett, P. C., Warren, S. J., Leggett, S. K., & Hodgkin, S. T. 2006, MNRAS, 367, 454

Luhman, K. L. 2012, ARA&A, 50, 65

Moorwood, A., et al. 1998, The Messenger, 94, 7

Patience, J., et al. 2012, A&A, 540, A85

Peña Ramírez, K., et al. 2012, ApJ, 754, 30

Perryman, M. A. C., et al. 1997, A&A, 323, L49

Saumon, D., et al. 1996, ApJ, 460, 993

Stephens, D. C., et al. 2009, ApJ, 702, 154

Zapatero Osorio, M. R., et al. 2002a, A&A, 384, 937

Zapatero Osorio, M. R., et al. 2002b, ApJ, 578, 536